Available online at www.sciencedirect.com
ScienceDirect
Journal of Power Sources 179 (2008) 329–334
JOURNAL OF POWER SOURCES
www.elsevier.com/locate/jpowsour

Short communication

Combustion synthesis of copper catalysts for selective CO oxidation

Nielson F.P. Ribeiro [a], Mariana M.V.M. Souza [a,b,*], Martin Schmal [a]

[a] *NUCAT/COPPE – UFRJ, Centro de Tecnologia, Bloco G, Sala 128, CEP 21945-970, Rio de Janeiro, RJ, Brazil*
[b] *Escola de Química – UFRJ, Centro de Tecnologia, Bloco E, Sala 206, CEP 21941-909, Rio de Janeiro, RJ, Brazil*

Received 5 December 2007; received in revised form 22 December 2007; accepted 31 December 2007
Available online 4 January 2008

Abstract

Copper catalysts supported on ceria, zirconia and niobia were prepared by combustion method with urea, containing a CuO loading of 6 wt.%, and tested on selective oxidation of CO. The characterization of the samples by X-ray diffraction (XRD) presented the formation of solid solution on CuO–CeO_2 catalyst and a change in crystalline structure of the support with copper insertion on ZrO_2 and Nb_2O_5 catalysts. The analysis of temperature-programmed reduction (TPR) revealed different interaction degrees of copper with the supports, with reduction peaks between 222 and 390 °C. The temperature-programmed desorption of CO (TPD-CO) profiles showed formation of CO_2 and H_2 only for the ceria and zirconia catalysts. In relation to the catalytic tests, the CuO–CeO_2 catalyst presented the best performance, with CO conversion of 95% at 150 °C up to 45 h on stream, and CO_2 selectivity of 55%.

Keywords: Copper; Ceria; Zirconia; Niobia; Selective oxidation; Carbon monoxide

1. Introduction

Selective CO removal from streams containing an excess of H_2 is the current challenge in heterogeneous catalysis research especially for preparation of H_2 suitable for proton exchange membrane fuel cell (PEMFC). The PEM fuel cells have attracted considerable attention for its application in transportation due to its low operation temperature, high efficiency and compactness [1,2]. Hydrogen is usually produced through steam reforming or partial oxidation of hydrocarbons or alcohols, followed by water–gas shift (WGS) reaction [3]. The effluent gases from such a process contain about 40–75% H_2, 15–25% CO_2, 0.5–2% CO, a few% H_2O and N_2 [4,5]. However, for use in PEMFC, CO levels have to be reduced to below 100 ppm and, preferably, 10 ppm, because of the poisoning of Pt–Ru electrocatalysts used as anode materials [6].

Several options for CO removal include palladium diffusion membranes, methanation and selective oxidation (SELOX) of CO [2,7]. Among the aforementioned methods, SELOX of CO is regarded as the most cost-effective, simplest and straightforward method. Therefore, the development of selective CO oxidation catalysts has stimulated considerable interest worldwide. The catalyst for the SELOX reaction must meet the requirements of high CO oxidation activity combined with high selectivity, to avoid the undesired H_2 oxidation side reaction. Another important requirement is that these catalysts should have good tolerance for CO_2 and H_2O in the feedstock.

The catalysts for SELOX of CO reported in the literature can be classified basically in three types: (a) noble metal catalysts (Pt, Pd, Rh supported on Al_2O_3, SiO_2 and zeolites) [8–11]. These catalysts exhibit good activity and stability in temperature range 150–250 °C, but the selectivity is not good enough to meet the practical requirements; (b) gold-based catalysts, which were much more active than Pt-group metal catalysts at low temperatures (<100 °C) but not so resistant towards deactivation by CO_2 and H_2O in the feed [12–14]; (c) several kinds of metal oxide catalysts, such as the oxides of Cu, Ni, Co, Mn alone or in combination [15,16]. Among these oxides, the CuO–CeO_2 mixed oxides have been shown as the most promising candidate

* Corresponding author at: Escola de Química – UFRJ, Centro de Tecnologia, Bloco E, Sala 206, Cidade Universitaria, CEP 21941-909, Rio de Janeiro, RJ, Brazil. Fax.: +55 21 25627598.
E-mail address: mmattos@eq.ufrj.br (M.M.V.M. Souza).

0378-7753/$ – see front matter © 2008 Elsevier B.V. All rights reserved.
doi:10.1016/j.jpowsour.2007.12.096

catalysts for SELOX of CO [17–21]. These catalysts are more active and selective than Pt-based catalysts while operating at significantly lower temperatures. When compared to Au-based catalysts, they are less active but much more selective and thermally stable [20,21]. Moreover, the absence of precious metals in their composition constitutes a great advantage in terms of cost, especially for transportation applications.

Fluorite oxides, such as CeO_2 and ZrO_2, are well known for their high oxygen mobility and high oxygen vacancy properties, which make them, appropriate candidates as oxidation catalyst components [22,23]. Niobia is also a reducible oxide, with considerable oxygen storage capacity [24,25]. Although CuO–CeO_2 and CuO–ZrO_2 catalysts have already been reported in the literature for SELOX of CO, CuO–Nb_2O_5 is a new system for this reaction, to our knowledge. In the present work we prepare CuO–CeO_2, CuO–ZrO_2 and CuO–Nb_2O_5 catalysts via the combustion method and examine their catalytic properties for SELOX of CO. The combustion method is an attractive technique for catalyst synthesis due to its low cost and simple preparation route, leading to homogeneous materials with nanocrystalline powders [26,27]. The samples were characterized by X-ray fluorescence (XRF), X-ray diffraction (XRD), temperature-programmed reduction (TPR) and temperature-programmed desorption of CO (TPD-CO). The results of this physicochemical characterization will be discussed in relation to the catalytic performance of the copper catalysts.

2. Experimental

2.1. Catalyst preparation

The CuO–CeO_2, CuO–ZrO_2 and CuO–Nb_2O_5 mixed oxide catalysts were prepared by urea–nitrate combustion method using a mixture of $Cu(NO_3)_2{\cdot}6H_2O$ (Vetec, Brazil), $Ce(NO_3)_2{\cdot}6H_2O$ (Aldrich), $ZrO(NO_3)_2{\cdot}6H_2O$ (Acros Organics) or $NH_4[NbO(C_2O_4)_2(H_2O)_2](H_2O)_n$ (CBMM, Brazil) in appropriate molar ratios. The mixture of the corresponding salts was melted on a hot plate (150 °C), and urea (Vetec, Brazil) was added to the molten reagents. The amount of urea was twice the theoretical amount, as determined by the propellant chemistry [26], to improve the crystallinity of the resulting powder. The basin was then introduced in a muffle furnace, preheated at 600 °C, where the combustion reaction took place. A rapid evolution of a large quantity of gases yielded a foamy, voluminous powder. Because the time for the autoignition is rather small (typically ≤5 s) [28], to remove traces of undecomposed urea, nitrates, and their decomposition products, the powders were calcined in flowing air at 600 °C for 3 h. The nominal CuO loading was 6.0 wt.%.

2.2. Catalyst characterization

The chemical composition of the synthesized samples was determined by X-ray fluorescence using a Rigaku spectrometer. X-ray powder diffraction patterns were recorded in a Rigaku miniflex X-ray diffractometer equipped with a graphite monochromator using Cu Kα radiation (40 kV).

The reducibility of the catalysts was analyzed by temperature-programmed reduction, carried out in a microflow reactor operating at atmospheric pressure. The samples were dehydrated at 150 °C under flowing Ar before the reduction. A mixture of 1.65% hydrogen in argon flowed at 30 mL min^{-1} through the sample, raising the temperature at a heating rate of 10 °C min^{-1} up to 700 °C. The outflowing gases were accompanied by a thermal conductive detector.

Temperature-programmed desorption of CO was carried out using a QMS-200 (BALZER) mass spectrometer. Prior to CO adsorption, the samples were reduced at 500 °C (10 °C min^{-1}) for 30 min using the mixture 10% H_2/He (30 mL min^{-1}) and then cooled to room temperature in He flow at 30 mL min^{-1}. Subsequently, the samples were exposed to CO atmosphere under flow of 10% CO/He for 1 h. Physisorbed CO was removed by purging He, and desorption was performed raising the temperature up to 500° (20 °C min^{-1}) in He flow (30 mL min^{-1}). The ratios m/e = 2, 12, 15, 16, 17, 18, 28, 32, and 44 were monitored.

2.3. Catalytic tests

Catalyst testing was performed in a flow tubular quartz reactor loaded with 100 mg of catalyst, under atmospheric pressure. The catalysts were reduced with 20% H_2/N_2 at 550 °C for 1 h. After reduction the catalyst was purged with nitrogen for 30 min at the same temperature. The total feed flow rate was held constant at 100 cm^3 min^{-1}, with 60% H_2, 1% CO, 1% O_2 and 38% He. The loss in catalyst activity was monitored up to 45 h on stream. The reaction products were analyzed by on-line gas chromatograph (Varian 3800), equipped with Poraplot Q and molecular sieve columns. The carrier gas was helium and it was used a thermal conductivity detector and methanizer followed by flame ionization detector.

CO and O_2 conversion and selectivity for CO_2 formation were defined as follows:

$$\text{CO conversion}\,(\%) = \frac{[\text{CO}]_{\text{in}} - [\text{CO}]_{\text{out}}}{[\text{CO}]_{\text{in}}} \times 100 \quad (1)$$

$$\text{O}_2\ \text{conversion}\ (\%) = \frac{[\text{O}_2]_{\text{in}} - [\text{O}_2]_{\text{out}}}{[\text{O}_2]_{\text{in}}} \times 100 \quad (2)$$

$$\text{CO}_2\ \text{selectivity}\ (\%) = \frac{0.5([\text{CO}]_{\text{in}} - [\text{CO}]_{\text{out}})}{[\text{O}_2]_{\text{in}} - [\text{O}_2]_{\text{out}}} \times 100 \quad (3)$$

3. Results and discussions

3.1. Catalyst characterization

The chemical composition of the catalysts is shown in Table 1. All the real copper loadings are very close to the

Table 1
Chemical composition of the catalysts

Catalyst	wt.% CuO	wt.% oxide
CuO–CeO_2	6.7	93.3
CuO–ZrO_2	6.9	93.1
CuO–Nb_2O_5	6.1	93.9

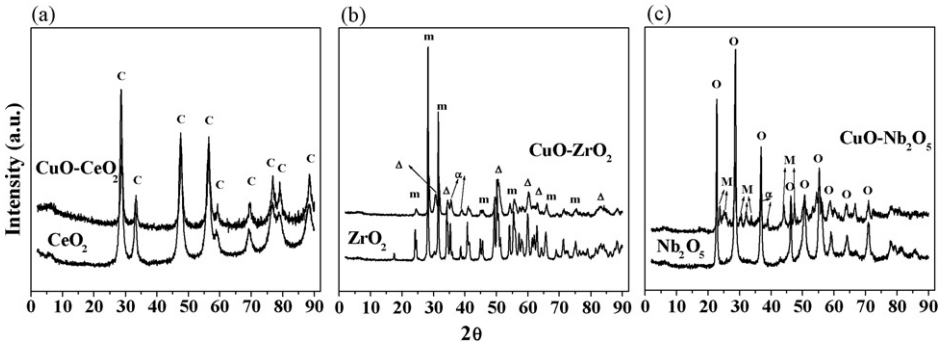

Fig. 1. X-ray diffractograms of the copper catalysts: (a) CuO–CeO_2, (b) CuO–ZrO_2 and (c) CuO–Nb_2O_5. C → CeO_2; α → CuO; m → ZrO_2 (monoclinic); Δ → ZrO_2 (tetragonal); O → Nb_2O_5 (orthorhombic); M → Nb_2O_5 (monoclinic).

nominal ones, showing that the preparation methodology was adequate.

The XRD patterns of the catalysts are presented in Fig. 1. For comparison, the corresponding patterns of the pure supports, prepared by the same combustion method, are also depicted.

For CuO–CeO_2 sample, XRD reflections characteristic of the fcc fluorite structure of CeO_2 (JCPDS 34-0394) are present in the pattern of both the support and catalyst. Diffraction lines due to CuO were not detected in CuO–CeO_2 catalyst, even when the 2θ region (30°–50°), where CuO peaks were expected, was expanded. Peaks due to Cu_2O were also not detected. The absence of copper oxide peaks may be attributed to highly dispersed CuO on the surface of ceria or the formation of Cu–Ce–O solid solution, or a combination of these two phenomena [4,27,29]. The formation of Cu–Ce–O solid solution was proposed by Bera et al. [30] based on Rietveld analysis of XRD spectra, which showed a reduction in the lattice parameter of ceria upon introduction of CuO, because the ionic radius of Cu^{2+} (0.76 Å) is smaller than that of Ce^{4+} (1.01 Å). Indeed, we observed a decrease in the cell parameter from 5.4193 Å in pure CeO_2 to 5.4028 Å in CuO–CeO_2, which confirms Cu^{2+} ion substitution in the CeO_2 matrix. Furthermore, the amount of Cu^{2+} incorporated into the CeO_2 lattice is lower than the nominal CuO loading, so that a part of Cu^{2+} resides on the catalyst surface, in accordance to Xiaoyuan et al. [31].

The XRD patterns of CuO–ZrO_2 catalyst (Fig. 1b) showed that ZrO_2 support consists of a mixture of monoclinic (JCPDS 37-1484) and tetragonal (JCPDS 42-1164) phases. The major peaks are due to the monoclinic-ZrO_2 phase, since the Rietveld analysis revealed 94% of monoclinic and 6% of tetragonal phase. After loading CuO, there was an increase in the contribution of tetragonal-ZrO_2 phase (29%) and the appearance of CuO-tenorite phase (JCPDS 48-1548). The crystallite size of CuO is 14.7 nm, calculated by Scherrer equation. Zhou et al. [32,33], studying CuO–ZrO_2 catalysts prepared by impregnation technique, also verified that at no copper loading, the major peaks were due to the monoclinic-ZrO_2 phase. With introduction of CuO, the tetragonal-ZrO_2 phase appeared in more peaks and increased with the copper loading. The monoclinic-ZrO_2 phase disappeared fully when CuO loading was higher than 10 wt.%.

For CuO–Nb_2O_5 catalyst, XRD patterns of pure Nb_2O_5 revealed only peaks due to orthorhombic phase (or T phase, according to Schäffer notation) (JCPDS 27-1003). Braga et al. [34,35] verified that niobium oxalate treated between 450 and 500 °C showed reflections compatible with hexagonal (TT) phase; above 500 °C, new reflections were observed, which may be attributed to orthorhombic (T) phase at 600 °C and a mixture of orthorhombic and monoclinic (M and H) phases at 800 °C. The addition of copper to niobia caused the appearance of the monoclinic-Nb_2O_5 phase (JCPDS 37-1468) and peaks due to tenorite CuO phase. The mean crystallite size of CuO is 25 nm, by Scherrer equation.

In order to assess the reduction behavior of the catalysts, TPR measurements were performed. Fig. 2 shows the TPR profiles of the catalysts.

The CuO–CeO_2 catalyst presented three overlapping reductions peaks at 222, 260 and 320 °C, which is an indication of the existence of more than one copper oxide species in this catalyst. The reduction of pure CuO is reported in the literature to occur between 290 and 390 °C [21,29,31]. Pure CeO_2, on the other hand, starts to get reduced at temperatures higher than 380–400 °C [27,36,37]. It is well known that ceria promotes the reduction of finely dispersed copper oxide surface species [23,27,30,31]. Xiaoyuan et al. [31] observed two reduction peaks in TPR profile of 5% CuO–CeO_2 prepared by impregnation method: the low temperature peak (∼200 °C) was related to the reduction of highly dispersed copper oxide species, whereas the high temperature peak (230 °C) to the reduction of the bulk CuO.

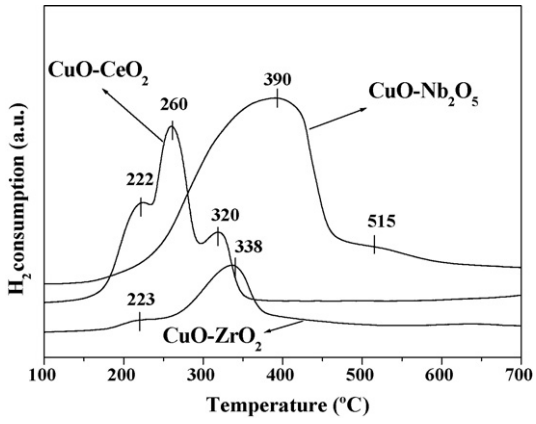

Fig. 2. TPR profiles of the copper catalysts.

These authors observed CuO diffraction peaks in their sample. In our case, we can attribute the low temperature peak (222 °C) to the reduction of the finely dispersed copper oxides on the surface of ceria and the peaks at higher temperatures (260 and 320 °C) to the reduction of copper ions in the CeO_2 matrix forming a solid solution, together with some reduction of ceria (the reduction degree was 137%, based on the real CuO loading determined by XRF).

The TPR profile of CuO–ZrO_2 shows a small peak at 223 °C and the main peak at 338 °C. No reduction peak was observed for ZrO_2 support alone. The two peaks in TPR profile of CuO–ZrO_2 may be attributed to the CuO species interacting differently with the ZrO_2 support. The low temperature peak may be ascribed to the highly dispersed CuO and/or Cu^{2+} ions with an octahedral environment, and the high temperature peak to the bulk CuO, according to Zhou et al. [32,33]. Ritzkopf et al. [38] verified by EXAFS of CuO/ZrO_2 that Cu^+ occurs as intermediate species during the reduction of the catalyst. Thus, the two peaks in TPR profile can be associated with the reduction of Cu^{2+} to Cu^0 on different copper particle sizes, probably with Cu^+ as intermediate species. There was an incomplete reduction of CuO, with reduction degree of only 79%.

CuO–Nb_2O_5 catalyst presented two reduction peaks in TPR profile: a broad and intense band at 390 °C and a small shoulder at 515 °C. The peak at 390 °C can be attributed to the reduction of CuO to Cu^0 together with the support reduction, because the reduction degree of CuO calculated by the integration of the peak area is higher than 100% (118%). Li et al. [39] observed a similar reduction temperature for Cu/Nb_2O_5 prepared by wetness impregnation and calcined at 600 °C. This temperature is considerable higher than that reported by Chary et al. [40] for Cu/Nb_2O_5 also prepared by impregnation and calcined at 500 °C: 216 °C for the first peak and 293 °C for the second one. The small shoulder at 515 °C is related to the additional reduction of niobia.

The TPD-CO spectra of the copper catalysts are given in Fig. 3. The CuO–CeO_2 catalyst showed a large desorption of CO_2 in two peaks, at 116 and 275 °C. There was also desorption of CO at 65 °C and a small formation of H_2, with peak maximum at 153 °C. The CO_2 desorption can be associated with the Boudouard reaction ($2CO \rightarrow CO_2 + C$) and/or the CO oxidation by the oxygen lattice of the support. Zou et al. [29] also carried out TPD-CO experiments for characterization of CuO/CeO_2 catalysts prepared by co-precipitation. They observed only one CO desorption peak at 162 °C and the profile did not go back to the original baseline, probably because they monitored the product gases by TCD. For CuO–ZrO_2 catalyst there was also a great desorption of CO_2, accompanied by desorption of H_2 with peak maxima at 146 and 249 °C. Besides the both hypothesis cited previously for CO_2 formation, it is also possible that CO reacts with hydroxyl groups of the support producing CO_2 and H_2. Interestingly, for CuO–Nb_2O_5 catalyst CO_2 desorption was very small and CO desorbed at 79 and 153 °C. This result is a good indicative of the low availability of the oxygen lattice for CO oxidation on CuO–Nb_2O_5.

3.2. Catalytic tests

The activity, in terms of CO and O_2 conversion, and CO_2 selectivity obtained with the copper catalysts for SELOX of CO in the presence of excess hydrogen are presented in Figs. 4 and 5, respectively. CO_2 and H_2O were the only reaction products; CH_4 formation was not observed. It is evident that the support has a strong influence on the catalytic performance.

The CuO–CeO_2 catalyst was the most active and selective, with CO conversion of 94% at 150 °C and CO_2 selectivity of 53% at this same temperature. The CuO–ZrO_2 and CuO–Nb_2O_5 catalysts were considerably less active, with maximum CO conversion of 25% at 250 °C and 30% at 150 °C, respectively. The decrease of selectivity with temperature is related to the mechanistic model involving CO and H_2 adsorption sites. At low temperatures (and high CO coverages) hydrogen adsorption and oxidation are practically inhibited, since limited by CO desorption. With increasing temperature, the CO coverage decreases, leading to a decline in selectivity due to increasing H_2 oxidation rate. Thus, the decrease in CO conversion is due to the increase in H_2 oxidation, since O_2 conversion always increases with temperature up to reach 100%.

The higher activity of CuO–CeO_2 catalyst can be attributed to the presence of highly dispersed CuO clusters in strong interaction with CeO_2, which is easily reduced at low temperatures, as demonstrated by TPR results. This is in agreement with other reports, which showed that the catalysts with the higher amount of easily reducible well-dispersed copper oxide on the surface of ceria were the most active for SELOX of CO [17,21,27]. The promotion effect of CeO_2 is due to the synergism of the

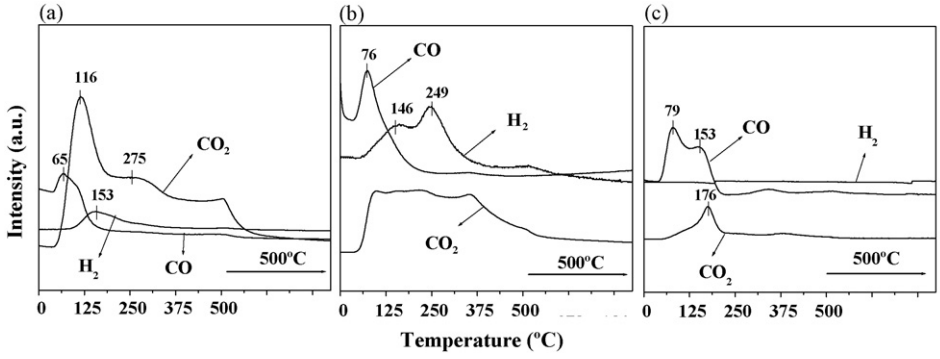

Fig. 3. TPD-CO profiles of the (a) CuO–CeO_2, (b) CuO–ZrO_2 and (c) CuO–Nb_2O_5 catalysts.

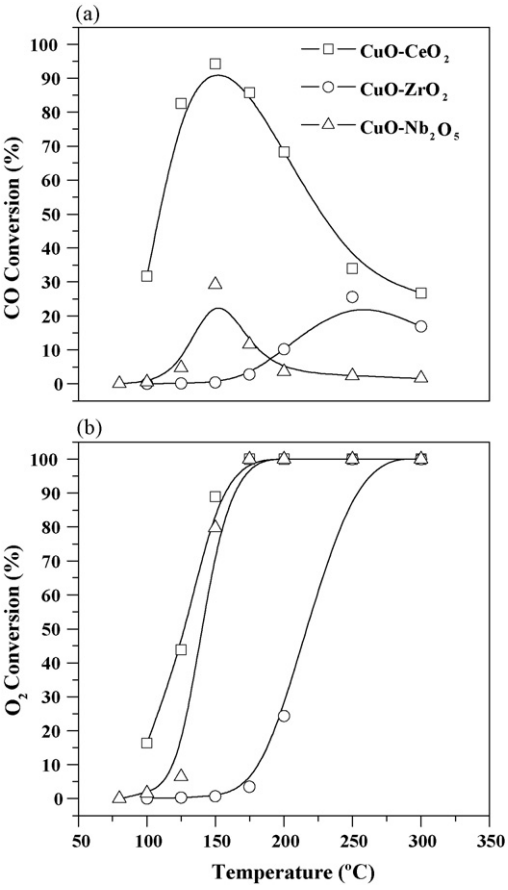

Fig. 4. Catalytic tests in terms of CO (a) and O_2 (b) conversions for the SELOX of CO over the copper catalysts.

redox properties of the system, achieved by the strong copper oxide–ceria interaction, which causes part of CuO to enter the CeO_2 lattice, forming solid solutions, and other part to disperse over the surface [27,31].

The CuO–ZrO_2 catalyst presented low activity, with activation at temperatures higher than 200 °C. This behavior can be associated with the presence of bulk CuO, which showed low interaction with zirconia and low reducibility. According to Ratnasamy et al. [36], while the isolated and dispersed CuO species exhibit reduction–oxidation behavior, the bulk CuO-like phase exhibits irreversible reduction behavior. And the amount of reducible and reoxidable CuO content is greater on CeO_2 than

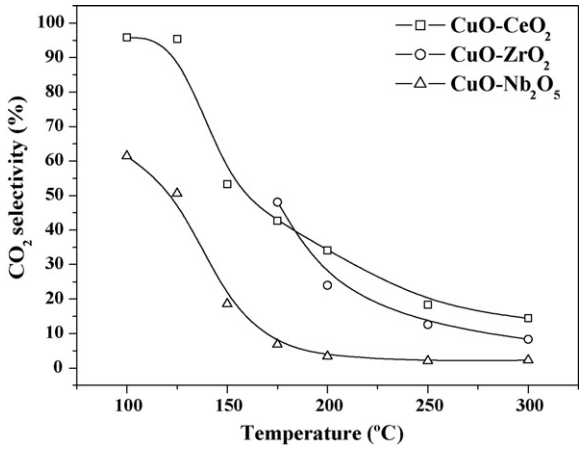

Fig. 5. CO_2 selectivity for the SELOX of CO over the copper catalysts.

on ZrO_2 catalysts. The low activity of the CuO–Nb_2O_5 catalyst can be related to its high reduction temperature (Fig. 2) and to the results of TPD-CO (Fig. 3), which showed small formation of CO_2 and, consequently, low activity of this catalyst for CO oxidation.

Deactivation tests were performed under the same conditions of the activity tests, at temperatures on which CO conversion reached the maximum value. Comparison of catalyst stabilities is shown in Fig. 6. The CuO–CeO_2 catalyst presented a very stable behavior, with 95% of CO conversion at 150 °C up to 45 h on stream. The CuO–ZrO_2 also presented a stable behavior, but with only 25% of CO conversion at 250 °C. The CuO–Nb_2O_5 catalyst showed a significantly deactivation on the first 2 h on stream at 150 °C, with CO conversion decreasing from 25% to 10%, followed by a gradual deactivation up to 36 h of reaction.

4. Conclusions

CuO–MO_x catalysts (M = Ce, Zr or Nb) were prepared by the combustion method with urea, characterized and tested on selective oxidation of CO. The CuO–CeO_2 sample exhibited the best catalytic performance, with CO conversion of 95% at 150 °C up to 45 h on stream. The CuO–ZrO_2 and CuO–Nb_2O_5 catalysts presented poor activity towards SELOX of CO with maximum CO conversion of only 25% at 250 °C and 30% at 150 °C, respectively.

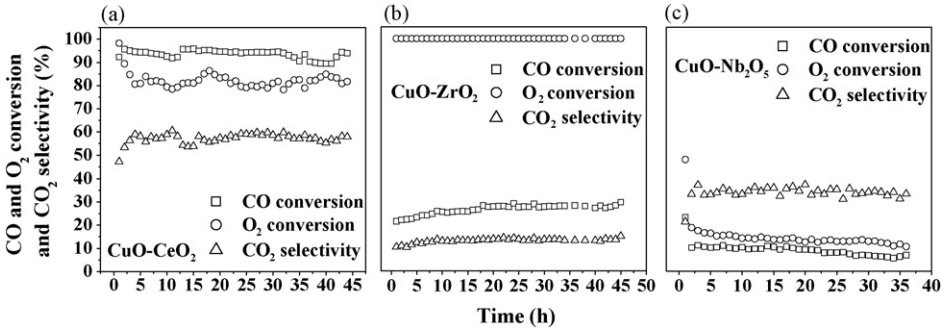

Fig. 6. Deactivation tests of the (a) CuO–CeO_2 at 150 °C, (b) CuO–ZrO_2 at 250 °C and (c) CuO–Nb_2O_5 at 150 °C.

As evidenced by the physicochemical characterization of the samples, for $CuO–CeO_2$ there was formation of easily reducible well-dispersed copper oxide species strongly interacting with the ceria surface. These species are responsible for the high activity of $CuO–CeO_2$ on SELOX of CO. The $CuO–ZrO_2$ and $CuO–Nb_2O_5$ catalysts presented formation of bulk CuO particles, with low interaction with the support and low reducibility. Moreover, $CuO–Nb_2O_5$ showed only a very small production of CO_2 during TPD-CO, indicating a low availability of the oxygen lattice of niobia for CO oxidation.

References

[1] C. Song, Catal. Today 77 (2002) 17–49.
[2] X.-F. Dong, H. Zou, W.-M. Lin, Int. J. Hydrogen Energy 31 (2006) 2337–2344.
[3] M.A. Peña, J.P. Gómez, J.L.G. Fierro, Appl. Catal. A: Gen. 144 (1996) 7–57.
[4] C.R. Jung, J. Han, S.W. Nam, T.-H. Lim, S.-A. Hong, H.-I. Lee, Catal. Today 93–95 (2004) 183–190.
[5] J.R. Rostrup-Nielsen, T. Rostrup-Nielsen, Cattech 6 (2002) 150–159.
[6] H.F. Oetjen, V.M. Schmidt, U. Stimming, F. Trila, J. Electrochem. Soc. 143 (1996) 3838–3842.
[7] S. Yamaguchi, S. Yamamoto, T. Shishido, M. Omori, A. Okubo, J. Power Sources 129 (2004) 4–6.
[8] S.H. Oh, R.M. Sinkenvitch, J. Catal. 142 (1993) 254–262.
[9] A. Manasilp, E. Gulari, Appl. Catal. B: Environ. 37 (2002) 17–25.
[10] P. Marques, N.F.P. Ribeiro, M. Schmal, D.A.G. Aranda, M.M.V.M. Souza, J. Power Sources 158 (2006) 504–508.
[11] M.M.V.M. Souza, N.F.P. Ribeiro, M. Schmal, Int. J. Hydrogen Energy 32 (2007) 425–429.
[12] R.J.H. Grisel, B.E. Nieuwenhuys, J. Catal. 199 (2001) 48–59.
[13] M.M. Schubert, V. Plzak, J. Garche, R.J. Behm, Catal. Lett. 76 (2001) 143–150.
[14] G.K. Bethke, H.H. Kung, Appl. Catal. A: Gen. 194 (2000) 43–53.
[15] K. Omata, T. Takada, S. Kasahara, M. Yamada, Appl. Catal. A: Gen. 146 (1996) 255–262.
[16] G.G. Xia, Y.G. Yin, W.S. Willis, J.Y. Wang, S.L. Suib, J. Catal. 185 (1999) 91–105.
[17] W. Liu, M. Flytzani-Stephanopoulos, J. Catal. 153 (1995) 304–316.
[18] W. Liu, M. Flytzani-Stephanopoulos, J. Catal. 153 (1995) 317–332.
[19] Y. Liu, Q. Fu, M.F. Stephanopoulos, Catal. Today 93-95 (2004) 241–246.
[20] G. Avgouropoulos, T. Ioannides, H.K. Matralis, J. Batista, S. Hocevar, Catal. Lett. 73 (2001) 3340.
[21] G. Avgouropoulos, T. Ioannides, H. Matralis, Appl. Catal. B: Environ. 56 (2005) 87–93.
[22] H.L. Tuller, P.K. Moon, Mater. Sci. Eng. B 20 (1988) 171–191.
[23] W. Liu, M. Flytzani-Stephanopoulos, Chem. Eng. J. 64 (1996) 283–294.
[24] T. Uchijima, Catal. Today 28 (1996) 105–117.
[25] D.A.G. Aranda, F.B. Noronha, F.B. Passos, M. Schmal, Appl. Catal. A: Gen. 100 (1993) 77–84.
[26] A. Ringuedé, J.A. Labrincha, J.R. Frade, Solid State Ionics 141 (2001) 549–557.
[27] G. Avgouropoulos, T. Ioannides, Appl. Catal. A: Gen. 244 (2003) 155–167.
[28] R.D. Purohit, B.P. Sharma, K.T. Pillai, A.K. Tyagi, Mater. Res. Bull. 36 (2001) 2711–2721.
[29] H. Zou, X. Dong, W. Lin, Appl. Surf. Sci. 253 (2006) 2893–2898.
[30] P. Bera, K.R. Priolkar, P.R. Sarode, M.S. Hegde, S. Emura, R. Kumashiro, N.P. Lalla, Chem. Mater. 14 (2002) 3591–3601.
[31] J. Xiaoyuan, L. Guanglie, Z. Renxian, M. Jianxin, C. Yu, Z. Xiaooming, Appl. Surf. Sci. 173 (2001) 208–220.
[32] R.-X. Zhou, T.-M. Yu, X.-Y. Jiang, F. Chen, X.-M. Zheng, Appl. Surf. Sci. 148 (1999) 263–270.
[33] R.-X. Zhou, X.-Y. Jiang, J.-X. Mao, X.-M. Zheng, Appl. Catal. A: Gen. 162 (1997) 213–222.
[34] V.S. Braga, F.A.C. Garcia, J.A. Fias, S.C.L. Dias, J. Catal. 247 (2007) 68–77.
[35] V.S. Braga, J.A. Dias, S.C.L. Dias, J.L. Macedo, Chem. Mater. 17 (2005) 690–695.
[36] P. Ratnasamy, D. Srinivas, C.V.V. Satyanarayana, P. Manikandan, R.S.S. Kumaran, M. Sachin, V.N. Shetti, J. Catal. 221 (2004) 455–465.
[37] G. Avgouropoulos, T. Ioannides, Appl. Catal. B: Environ. 67 (2006) 1–11.
[38] I. Ritzkopf, S. Vukojević, C. Weidenthaler, J.-D. Grunwaldt, F. Schüth, Appl. Catal. A: Gen. 302 (2006) 215–223.
[39] J. Li, G. Lu, K. Li, W. Wang, J. Mol. Catal. A 221 (2004) 105–112.
[40] K.V.R. Chary, K.K. Seela, G.V. Sagar, B. Sreedhar, J. Phys. Chem. B 108 (2004) 658–663.